

# Energy-based Control for Soft Manipulators using Cosserat-beam Models

Brandon Caasenbrood<sup>1</sup> <sup>a</sup>, Alexander Pogromsky<sup>1,2</sup> <sup>b</sup> and Henk Nijmeijer<sup>1</sup> <sup>c</sup>

<sup>1</sup>*Department of Mechanical Engineering, Eindhoven University of Technology, The Netherlands*

<sup>2</sup>*Department of Control Systems and Informatics, Saint-Petersburg National Research University of Information Technologies, Mechanics, and Optics (ITMO), Russian Federation*

**Keywords:** Soft Robotics, Cosserat Beam Theory, Dynamic Modeling, Energy-based Control.

**Abstract:** In this work, we describe an energy-based control method for under-actuated soft manipulators. The continuous dynamics of the soft robot are modeled by the differential geometry of Cosserat beams. Through a finite-dimensional truncation, a reduced port-Hamiltonian model is obtained that preserves desirable passivity conditions. Exploiting the passivity, we propose a stabilizing energy-shaping controller that ensures the potential energy is minimal at the desired end-effector configuration. Finally, the effectiveness of the energy-based controller is demonstrated through simulations of a soft manipulator inspired by the tentacle of an octopus.


## 1 INTRODUCTION


With an origin in material science, soft robotics is slowly vesting itself as a prominent successor to conventional rigid robotics. Unlike traditional robots, soft robots are composed of ‘*soft materials*’ that enable a rich family of motion primitives, inherent safety, and robustness towards environmental uncertainties. By fully exploiting the properties in soft materials, soft robotics places the first stepping stones towards achieving performance similar to biology (Choi et al., 2011; Falkenhahn et al., 2015; Marchese et al., 2014; Kriegman et al., 2019). In this paper, we primarily focus on a particular subclass of soft robotics – soft robot manipulators.


Although significant steps have been taken towards bridging biology and soft robotics, its innate infinite-dimensionality poses substantial challenges on modeling and control. In theory, soft robots possess infinitely many degrees-of-freedom along their continuously deformable body, rendering them particularly suited for Partial Differential models. Besides, their mechanical design often employs distributed actuation (e.g., pneumatics and tendons). Classical descriptions of rigid links and joints paired with localized actuation are therefore no longer viable nor

physically representative. This paradigm shift calls for new control-oriented modeling approaches suited for these intrinsically hyper-redundant and under-actuated robotic systems.

In the last decade, modeling approaches for soft robot manipulators have matured sufficiently and as such their applicability in model-based control is slowly realizable. To highlight a few: reduced-order finite element models (Duriez, 2013; Zhang et al., 2017), constant and non-constant curvature approaches (Katzschmann et al., 2019; Della Santina and Rus, 2020), Cosserat-beam models (Renda et al., 2020; Boyer et al., 2020), modal approximations (Chirikjian and Burdick, 1992), and learning-based approaches (Thuruthel et al., 2018). Among them, the Piece-wise Constant Curvature (PCC) model remains one of the most favored techniques of spatial reduction. The PCC model has proven to be viable for applications like feedforward controllers (Falkenhahn et al., 2015), and more recently feedback dynamic controllers (Della Santina and Rus, 2020; Katzschmann et al., 2019). Nevertheless, the approach has its limitations. They do not originate from continuum mechanics and thus are only applicable in restrictive settings. Although they offer better computational performance than continuous models, due to their kinematic restrictions, they are unable to capture important continuum phenomena, like buckling, environmental interaction or wave propagation.

<sup>a</sup>  <https://orcid.org/0000-0002-6299-1730>

<sup>b</sup>  <https://orcid.org/0000-0001-8755-9832>

<sup>c</sup>  <https://orcid.org/0000-0001-5883-6191>

Cosserat beam-models, on the other hand, have shown to capture a wider range of nonlinear continuum deformations. These models are rooted in continuum mechanics and thus provide a more accurate description of the hyper-flexible nature of soft robots. The computational dynamics of Cosserat beams have been extensively developed by (Simo and Vu-Quoc, 1986) through Geometrically-Exact finite elements on the Lie group  $SE(3)$ ; and recently, these models are slowly gaining popularity in the soft robotics community (Renda et al., 2020; Boyer et al., 2020; Till et al., 2019). Ultimately, the strong nonlinearities paired with the diligence to achieve biological performance encourage Cosserat models for feedback control. Yet, to the author's knowledge, their application on model-based feedback control is relatively scarce.

In this work, we aim to highlight the capabilities of Cosserat models for model-based control, in particular energy-based strategies. To this end, a finite-dimensional modeling approach is proposed such that the continuous dynamics can be cast into a port-Hamiltonian (pH) structure. The main advantage of pH systems is the common formalism with energy-based control. Through the pH structure, we propose an energy-shaping control law that ensures stabilization of the end-effector of the soft robot. Similar energy-based control strategies can be found in (Franco and Garriga-Casanovas, 2020; Schaft, 2004; Ortega et al., 2002) for rigid-body systems. As a study case, we consider a soft robot manipulator inspired by an octopus tentacle (see Figure 1). With the ability to deform continuously and its distributed muscular system, it is ideal for illustrating the complex morphological motions present in soft robotics. All source code is made publicly available at (Caasenbrood, 2020).

The paper is organized as follows. Section 2 will detail a modeling approach for a general class of soft robot manipulators, starting with the Cosserat-beam theory. In Section 3, we propose an energy-shaping control strategy. Lastly, we show the effectiveness of energy-based controller through numerical simulation, followed by a brief conclusion in Section 5.

## 2 DYNAMIC MODELING

### 2.1 Lie Group Notations

Throughout this work, we will explore Lie group theory. We introduce the following notations: the Lie group of rigid-body transformation on  $\mathcal{R}^3$  is denoted by  $SE(3)$ , whereas the group of homogeneous rotation is denoted by  $SO(3)$ . The tangent space at the identity of the group is called the Lie algebra, and it

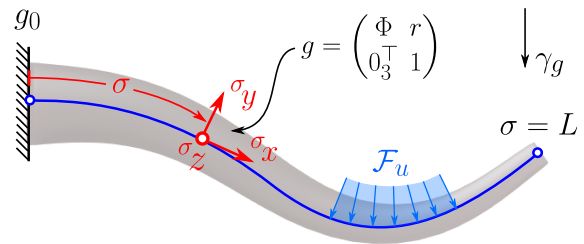


Figure 1: Schematic representation of a soft robot manipulator inspired by the tentacle of an octopus. The soft robot is modeled as a Cosserat beam with distributed actuation  $\mathcal{F}_u$ .

can be used to describe the evolution of the Lie group. The Lie algebra of  $SE(3)$  and  $SO(3)$  are denoted by  $se(3)$  and  $so(3)$ , respectively. Lastly, the cross operator (i.e., " $\times$ ") and hat operator (i.e., " $\wedge$ ") are used to transform a column vector of  $\mathcal{R}^3$  or  $\mathcal{R}^6$  into an element of the Lie algebra  $so(3)$  or  $se(3)$ , respectively.

### 2.2 Cosserat Beam Theory

In Cosserat theory, slender deformable solids are modeled as elastic strings subjected to geometric finite-strain theory. Drawing the analogy to soft robotics, we model the soft robot as a one-dimensional spatial curve passing through the geometric center of the soft robot (see Figure 1). We call this curve the '*backbone curve*'. Given its spatio-temporal nature, we introduce a temporal variable  $t \in [0, T]$  with finite horizon time  $T$ , and a spatial variable  $\sigma \in [0, L]$  with  $L$  the undeformed length of the soft robot. For convenience, we denote  $\mathbb{T} = [0, T]$  and  $\mathbb{X} = [0, L]$ . For each point on the backbone, we introduce a (mobile) Serret-Frenet frame that is spanned by a basis of orthonormal vectors  $\{\sigma_x, \sigma_y, \sigma_z\}$ . The homogeneous rotation related to these Serret-Frenet frames is given by the rotation matrix  $\Phi(\sigma, t) \in SO(3)$ , and their origin by the position vector  $r(\sigma, t) \in \mathcal{R}^3$ .

Following the geometric approach (Simo and Vu-Quoc, 1986; Boyer et al., 2010; Renda et al., 2020), we may equivalently represent all Serret-Frenet frames that are rigidly attached to the continuous backbone by a parameterized curve in  $SE(3)$ :

$$g(\sigma, t) := \begin{pmatrix} \Phi(\sigma, t) & r(\sigma, t) \\ 0_3^T & 1 \end{pmatrix} \in SE(3). \quad (1)$$

By considering the partial derivatives of  $g$ , an expression for the strain field  $\xi$  and velocity field  $\eta$  anywhere on the Cosserat beam can be found in terms of its Lie algebra  $se(3)$ . To do so, we have to introduce some smoothness conditions:

**Assumption 1.** All control inputs, i.e., a distributed control wrench acting on the system, are considered to be sufficiently smooth for any instance  $t \in \mathbb{T}$  and  $\sigma \in$

$\mathbb{X}$  such that the resulting backbone  $g(\sigma, t) \in SE(3)$  is everywhere differentiable.

### 2.3 Local Strain and Velocity

Let  $\Gamma = (\kappa_1, \kappa_2, \kappa_3)^\top$  and  $U = (v_1, v_2, v_3)^\top$  be the torsion-curvature and elongation-shear strain vector, respectively. Then, an expression for strain field  $\xi(\sigma, t)$  is obtained through spatial differentiation of  $g$ :

$$\hat{\xi} := g^{-1} \frac{\partial g}{\partial \sigma} = \begin{pmatrix} \Gamma^\times & U \\ 0_3^\top & 0 \end{pmatrix} \implies \xi := \begin{pmatrix} \Gamma \\ U \end{pmatrix}, \quad (2)$$

Similarly, let  $\Omega = (\omega_1, \omega_2, \omega_3)^\top$  and  $V = (v_1, v_2, v_3)^\top$  be the angular and linear velocity vector, respectively. Then, an expression for velocity field  $\eta(\sigma, t)$  is obtained through time differentiation of  $g$ :

$$\hat{\eta} := g^{-1} \frac{\partial g}{\partial t} = \begin{pmatrix} \Omega^\times & V \\ 0_3^\top & 0 \end{pmatrix} \implies \eta := \begin{pmatrix} \Omega \\ V \end{pmatrix}. \quad (3)$$

Since we assume  $g$  to be everywhere differentiable, we can derive a PDE relation for the continuous forward kinematics of the soft robot:

$$\frac{\partial \eta}{\partial \sigma} = -\text{ad}_\xi \eta + \hat{\xi}, \quad (4)$$

where  $\text{ad}_{(\cdot)} : \mathcal{R}^6 \mapsto \mathcal{R}^{6 \times 6}$  denotes the adjoint action on the Lie algebra (full derivation in Appendix A). For completeness, we introduce the adjoint action on the group and its algebra by

$$\text{Ad}_g := \begin{pmatrix} \Phi & 0 \\ r^\times \Phi & \Phi \end{pmatrix}; \quad \text{ad}_\xi := \begin{pmatrix} \Gamma^\times & 0 \\ U^\times & \Gamma^\times \end{pmatrix}, \quad (5)$$

respectively. Drawing an analogy to rigid robotics, the expression in (4) may be seen as the forward velocity kinematics for a serial chain robot manipulator with infinitely many links. The expressions for the Cosserat beam kinematics above is derived similarly in (Boyer et al., 2020) and (Renda et al., 2020).

### 2.4 Finite-dimensional Reduction

Similar to finite element methods, we wish to find a finite-dimensional approximation of the strain field  $\xi(\sigma, \cdot)$  for all points on the material domain  $\mathbb{X}$ . To do so, we assume the following:

**Assumption 2.** Any element of the strain field  $\xi(\sigma, t)$  can be written as an infinite expansion of the following form:

$$\xi_i(\sigma, t) = \sum_{n=1}^{\infty} \theta_n(\sigma) q_{i,n}(t) + \xi_i^\circ(\sigma) \quad i \in \{1, \dots, 6\}, \quad (6)$$

where  $\{\theta_n\}_{n=1}^{\infty}$  is the set of basis functions  $\theta_n : \mathbb{X} \rightarrow \mathcal{R}$  together with modal coefficients  $q_{i,n} : \mathbb{T} \rightarrow \mathcal{R}$ , and an intrinsic time-invariant strain  $\xi_i^\circ : \mathbb{X} \rightarrow \mathcal{R}$ . The basis functions  $\theta_n(\cdot)$  and the modal coefficients  $q_n(\cdot)$  are both smooth functions.

**Assumption 3.** Given (6), the  $k$ -th order truncation for an element of the strain field, defined as

$$[\xi_i]_k(\sigma, t) := \sum_{n=1}^k \theta_n(\sigma) q_{i,n}(t) + \xi_i^\circ(\sigma) \quad i \in \{1, \dots, 6\}, \quad (7)$$

converges uniformly on  $\mathbb{T}$  and  $\mathbb{X}$  as the index  $k \rightarrow \infty$ . Moreover, we assume that uniform convergence holds for its partial derivatives  $\frac{\partial}{\partial t} [\xi]_k$  and  $\frac{\partial}{\partial \sigma} [\xi]_k$ .

Accordingly, we can rewrite the  $k$ -th order truncation of the complete strain field as follows

$$\begin{aligned} [\xi]_k &= (I_6 \otimes [\theta_1 \quad \dots \quad \theta_k]) q + \xi^\circ, \\ &= \underbrace{\begin{pmatrix} \theta_1 & \dots & \theta_k & \dots & 0 & \dots & 0 \\ \vdots & \ddots & \vdots & \ddots & \vdots & \vdots & \vdots \\ 0 & \dots & 0 & \dots & \theta_1 & \dots & \theta_k \end{pmatrix}}_{\Theta(\sigma)} \begin{pmatrix} q_{1,1} \\ \vdots \\ q_{6,k} \end{pmatrix} + \xi^\circ, \quad (8) \end{aligned}$$

where  $\Theta \in \mathcal{R}^{6 \times 6k}$  is a sparse shape function matrix with mutually orthogonal columns, the operator  $\otimes$  denotes the Kronecker product, and the vector  $q \in \mathcal{R}^{6k}$  is the collection of all time-variant modal coefficients. Although a wide variety of bases are possible (Boyer et al., 2020; Della Santina and Rus, 2020), we have chosen a modified Legendre polynomial set:

$$\theta_n(\sigma) = \frac{2}{2^n(n-1)!} \frac{d^{n-1}}{d\sigma^{n-1}} \left[ \left( \frac{2\sigma}{L} - 1 \right)^2 - 1 \right]^{n-1} \quad (9)$$

with  $n \in \mathbb{Z}^+$  the polynomial degree. An alternative option could be constructing the set of basis functions through the so-called 'snapshot decomposition method' using FEM-driven data (Astrid et al., 2008).

### 2.5 Finite-dimensional Kinematics

Given the finite-dimensional truncation in (8), we can now find an expression for the finite-dimensional forward kinematics in terms of the generalized coordinates  $q$  and its velocities components  $\dot{q}$ .

First, let us regard the configuration of the soft robot  $g \in SE(3)$ . Recall that the spatial evolution of the configuration is described by  $\partial g / \partial \sigma = g \hat{\xi}^\wedge$ , see Eq. (2). Given the initial condition  $g(0, \cdot) = g_0$ , an approximation of the continuously deformable soft robot can be obtained by partial integration over the spatial domain:

$$[g]_k(\sigma, t) = g_0 \int_0^\sigma [\hat{\xi}]_k(s, t) ds. \quad (10)$$

Next, let's regard the velocity kinematics  $\eta(\sigma, t)$  for any point  $\sigma$  on the backbone curve. Using the differential property of the adjoint action  $\text{ad}_\xi = -\partial/\partial\sigma[\text{Ad}_{g^{-1}}]\text{Ad}_g$  (Murray et al., 1994), we can rewrite the continuous forward kinematics in (4) as

$$\frac{\partial\eta}{\partial\sigma} = \frac{\partial}{\partial\sigma} (\text{Ad}_{g^{-1}}) \text{Ad}_g \eta + \dot{\xi}. \quad (11)$$

Now, given the initial condition  $\eta(0, \cdot) = 0_6$  and the approximations  $[\xi]_k$  and  $[g]_k$ , we can find an approximation to the velocity twist  $\eta$  by partial integration over space:

$$[\eta]_k(\sigma, t) = \text{Ad}_{[g]_k^{-1}} \int_0^\sigma \text{Ad}_{[g]_k} \Theta ds \dot{q} := [J]_k \dot{q}, \quad (12)$$

which naturally gives rise to the geometric Jacobian  $[J]_k \in \mathcal{R}^{6 \times 6k}$ . The geometric Jacobian plays an important role in obtaining the Lagrangian form of the reduced-order dynamic model. Finally, to express the acceleration twist, we take the time-derivative of (12) leading to

$$\begin{aligned} [\dot{\eta}]_k &= [J]_k \ddot{q} + [\dot{J}]_k \dot{q}, \\ &= [J]_k \ddot{q} + \text{Ad}_{[g]_k^{-1}} \int_0^\sigma \text{Ad}_{[g]_k} \text{ad}_{[\eta]_k} \Theta ds \dot{q}, \end{aligned} \quad (13)$$

which gives rise to the analytic expression of the time-derivative of the geometric Jacobian  $[\dot{J}]_k$  (see Appendix B for the derivation).

## 2.6 Finite-dimensional Dynamics

Here, we detail the dynamics of the Cosserat beam. First, let us consider an infinitesimal slice of continuum body that is perpendicular to the backbone curve. The kinetic momenta of this infinitesimal slice is then given by  $\mu(\sigma, t) = \mathcal{M}\eta(\sigma, t)$  in which  $\mathcal{M} \in se^*(3) \times se(3) \cong \mathcal{R}^{6 \times 6}$  denotes the symmetric inertia tensor.

**Remark 1.** For some soft robots, the inertia tensor  $\mathcal{M}$  may have an explicit dependency on space or time (or both). Nevertheless, for sake of simplicity, we limit ourselves to a diagonal invariant inertia tensor  $\mathcal{M} = \text{diag}\{\rho I_3, \rho \mathcal{A}\}$  with line-density  $\rho > 0$  and the second moment of area  $\mathcal{A} \in so^*(3) \times so(3) \cong \mathcal{R}^{3 \times 3}$ .

Using the expression of the kinetic momenta  $\mu$  of the infinitesimal body, we can write the equation of motion for a particular slice at  $\sigma$  using the Newton-Euler equations:

$$\frac{\partial}{\partial t} (\text{Ad}_{g^{-1}} \mu) = \text{Ad}_{g^{-1}} \mathcal{F}, \quad (14)$$

where again  $\text{Ad}_{(\cdot)}$  stands for the adjoint action on the Lie group, and  $\mathcal{F} = \mathcal{F}_c + \mathcal{F}_u - \mathcal{F}_g - \mathcal{F}_e$  the resultant wrench that is composed of the constraint wrench

$\mathcal{F}_c$ , the input wrench  $\mathcal{F}_u$ , and the potential wrenches due to gravity and visco-elasticity,  $\mathcal{F}_g$  and  $\mathcal{F}_e$ , respectively. Further evaluation of (14) leads to

$$\mathcal{M}\dot{\eta} - \text{ad}_\eta^\top \mathcal{M}\eta = \mathcal{F}, \quad (15)$$

where we used the fact that  $\text{Ad}_g^{-1} = -\text{ad}_\eta \text{Ad}_g^{-1}$ . Before continuing, we introduce a slight modification to the relation above. Using the fact that  $\text{ad}_\eta \eta = 0_6$ , we can introduce the vector  $\mathcal{M}\text{ad}_\eta \eta$  to (15) without affecting the dynamics. The importance of this modification originates from the preservation of passivity in the Lagrangian model, which is an important property in stability theorems for robotics. By substitution of the null vector, the equation of motion becomes

$$\mathcal{M}\dot{\eta} + (\mathcal{M}\text{ad}_\eta - \text{ad}_\eta^\top \mathcal{M})\eta = \mathcal{F}, \quad (16)$$

which is nothing more than the Newton-Euler equation for rigid-body motion on  $\mathcal{R}^3$ . To introduce the (reduced-order) Cosserat kinematics and make the expression symmetric, we substitute (12) and (13) into (16) and pre-multiply by  $[J]_k^\top$ :

$$\begin{aligned} [J]_k^\top (\mathcal{M}[J]_k \ddot{q} + \mathcal{M}[\dot{J}]_k \dot{q} + C_{[\eta]_k} \dot{q}) \\ = [J]_k^\top (\mathcal{F}_u - \mathcal{F}_g - \mathcal{F}_e), \end{aligned} \quad (17)$$

where  $C_{(\cdot)} = -C_{(\cdot)}^\top := \mathcal{M}\text{ad}_{(\cdot)} - \text{ad}_{(\cdot)}^\top \mathcal{M}$  is a skew-symmetric matrix. It is important to note that by pre-multiplication of the transpose Jacobian, we have eliminated the constraint wrenches, i.e.,  $[J]_k^\top \mathcal{F}_c = 0_6$  (Murray et al., 1994). Finally, the finite-dimensional dynamics of the deformable soft robot is found by spatial integration of (16) over the material domain  $\mathbb{X}$ . The overall dynamics can be written in familiar Euler-Lagrangian (EL) form as follows

$$M(q)\ddot{q} + C(q, \dot{q})\dot{q} + N(q) + F(q, \dot{q}) = \tau(q, t) \quad (18)$$

with the system matrices:

$$M(q) = \int_{\mathbb{X}} [J]_k^\top \mathcal{M} [J]_k d\sigma, \quad (19)$$

$$C(q, \dot{q}) = \int_{\mathbb{X}} [J]_k^\top \mathcal{M} [\dot{J}]_k + [J]_k^\top C_{[\eta]_k} [J]_k d\sigma, \quad (20)$$

$$N(q) = \int_{\mathbb{X}} [J]_k^\top \mathcal{F}_g d\sigma, \quad (21)$$

$$F(q, \dot{q}) = \int_{\mathbb{X}} [J]_k^\top \mathcal{F}_e d\sigma := Kq + D\dot{q}, \quad (22)$$

$$\tau(q, t) = \int_{\mathbb{X}} [J]_k^\top \mathcal{F}_u d\sigma := Gu(t), \quad (23)$$

where  $M$  is the generalized inertia matrix,  $C$  the centripetal-Coriolis matrix,  $N$  a vector of generalized potential forces with  $\mathcal{F}_g = -\text{Ad}_{[g]_k^{-1}} \mathcal{M}\gamma_g$  the external wrench acting on the body due to gravitational acceleration  $\gamma_g$ , and  $F_k$  a vector of viscoelastic forces imposed by the stiffness matrix  $K$  and damping matrix

*D.* The vector  $Gu$  represents the distributed forces and torques generated by various kinds of the internal actuators (e.g., tendons or pneumatics). If  $\text{rank}(G) < \dim(q)$ , the system is considered to be under-actuated. Within the context of soft robotics, whose infinite-dimensional configuration space cannot be matched by a finite number of actuators, these systems are often intrinsically under-actuated. Following the procedures in finite elements and assuming linear viscoelasticity, the stiffness matrix and damping matrix are computed through spatial integration:

$$K = \int_{\mathbb{X}} \Theta^\top \mathcal{K} \Theta d\sigma, \quad (24)$$

$$D = \int_{\mathbb{X}} \Theta^\top \mathcal{D} \Theta d\sigma, \quad (25)$$

where  $\mathcal{K} \in se^*(3) \times se(3)$  and  $\mathcal{D} \in se^*(3) \times se(3)$  are the stiffness and damping tensor, respectively.

**Lemma 1.** *The inertia matrix  $M(q)$  is a symmetric, positive definite, symmetric, and is uniformly bounded such that there exists constants  $\lambda_1 < \lambda_2$  such that  $\lambda_1(q)I_n \preceq M(q) \preceq \lambda_2(q)I_n < \infty$ .*

*Proof.* Proof can be found in (Spong et al., 2006)  $\square$

**Lemma 2.** *Given the inertia matrix  $M(q)$  and the Coriolis matrix  $C(\dot{q}, q)$  as described by (19) and (20), respectively, it can be shown that the matrix  $\dot{M} - 2C$  is skew-symmetric.*

*Proof.* To show  $\dot{M} - 2C$  is skew-symmetric, we start by computing the time-derivative of the inertia matrix. For sake of clarity, let's abbreviate  $[J]_k = J$  and  $[\dot{J}]_k = \dot{J}$ . Through chain differentiation, we find

$$\dot{M} = \int_{\mathbb{X}} \dot{J}^\top \mathcal{M} J + J^\top \mathcal{M} \dot{J} d\sigma, \quad (26)$$

Then, calculating  $\dot{M} - 2C$  leads to

$$\dot{M} - 2C = \int_{\mathbb{X}} \dot{J}^\top \mathcal{M} J - J^\top \mathcal{M} \dot{J} - 2J^\top C J d\sigma. \quad (27)$$

Since  $J^\top C J$  is skew-symmetric, the remainder of the proof consists of showing that the matrix  $S = \dot{J}^\top \mathcal{M} J - J^\top \mathcal{M} \dot{J}$  also satisfies skew-symmetry. Since  $\mathcal{M} = \mathcal{M}^\top$ , we can easily show this holds true:

$$\begin{aligned} S &= \dot{J}^\top \mathcal{M}^\top J - J^\top \mathcal{M}^\top \dot{J}, \\ &= -\left(\dot{J}^\top \mathcal{M}^\top J - J^\top \mathcal{M} \dot{J}\right)^\top = -S^\top. \end{aligned} \quad (28)$$

Therefore, the matrix  $\dot{M} - 2C$  is skew-symmetric.  $\square$

In literature, Lemma 2 is often referred to as the passivity condition. It implies that, in the absence of external dissipation, the total energy of the system (i.e., the Hamiltonian) is conserved. It shall be clear

that the passivity property is an important means of proving stability for robotic systems. It is also worth mentioning that this condition does not necessarily hold true for all cases, only for particular computations of the Coriolis matrix  $C(q, \dot{q})$  (e.g., through the Christoffel symbols).

## 2.7 port-Hamiltonian Formulation

In this section, the Lagrangian model in (18) is rewritten in port-Hamiltonian form. To this end, we define the generalized momenta  $p := M\dot{q}$ . Then, the (reduced-order) Hamiltonian is given by  $\mathcal{H} = \mathcal{T} + \mathcal{V}$  with  $\mathcal{T}(p, q) = \frac{1}{2}p^\top M^{-1}p$  and  $\mathcal{V}(q)$  the kinetic and potential energy of reduced system, respectively.

Given the Hamiltonian  $\mathcal{H}$ , it can be easily shown that generalized velocities can be written in terms of partial derivatives of the Hamiltonian function

$$\dot{q} = \frac{\partial \mathcal{H}}{\partial p} = M^{-1}p. \quad (29)$$

Note that  $M^{-1}$  exists due to the positive definiteness condition in Lemma 1. Similarly, we aim to find a differential equation that relates the time evolution of  $p$  to the Hamiltonian. Applying the chain rule of differentiation to the generalized momenta  $p$ , we find

$$\begin{aligned} \dot{p} &= \dot{M}\dot{q} + M\ddot{q}, \\ &= (\dot{M} - C - D)M^{-1}p - Kq - N + Gu, \end{aligned} \quad (30)$$

Taking the partial derivative of the Hamiltonian  $\mathcal{H}$  with respect to the generalized coordinates  $q$ , we find

$$\frac{\partial \mathcal{H}}{\partial q} = \frac{1}{2} \frac{\partial}{\partial q} \left( \dot{q}^\top M(q) \dot{q} \right) + \frac{\partial \mathcal{V}}{\partial q}. \quad (31)$$

To relate (30) and (31), we have to exploit some structural properties in the Lagrangian model. To be more specific, we exploit the skew-symmetry condition as detailed in Lemma 2. According to the (Spong et al., 2006), if the matrix  $S = \dot{M} - 2C$  satisfies the passivity condition in Lemma 2, it can be shown that

$$S\dot{q} = -\frac{\partial}{\partial q} \left( \dot{q}^\top M(q) \dot{q} \right) - \dot{M}\dot{q}. \quad (32)$$

Finally, by combining (29), (30), (31), and (32), we can show that the Lagrangian model in (18) can be equivalently rewritten as a port-Hamiltonian system:

$$\begin{cases} \dot{q} = \frac{\partial \mathcal{H}}{\partial p}, \\ \dot{p} = -\frac{\partial \mathcal{H}}{\partial q} - D \frac{\partial \mathcal{H}}{\partial p} + Gu. \end{cases} \quad (33)$$

with the reduced-order Hamiltonian  $\mathcal{H} = \frac{1}{2}p^\top M^{-1}p + \mathcal{V}$ . The advantage of the port-Hamiltonian model over the EL structure in (18) is the general applicability to different physical domains and the common formalism with energy-based control techniques.

### 3 ENERGY-BASED CONTROL

In this section, we aim to find a control law  $u$  that ensures  $\lim_{t \rightarrow \infty} g(L, t) = g_d$  where  $g_d \in SE(3)$  denotes the desired configuration of the end-effector. To achieve the control objective, the idea is to shape the potential energy of the reduced-order dynamical system using conventional energy-shaping techniques from the port-Hamiltonian control theory.

#### 3.1 Energy-shaping Controller

We adopted an energy-based control strategy akin to the work of (Ortega et al., 2002) and (Franco and Garriga-Casanovas, 2020). Following a similar energy-shaping strategy, the nonlinear controller takes the form

$$u = G^+ \left( \frac{\partial \mathcal{H}}{\partial q} - \frac{\partial \mathcal{H}_d}{\partial q} \right), \quad (34)$$

where  $G^+ = (G^\top G)^{-1} G^\top$  is the generalized inverse of  $G$ , and  $\mathcal{H}_d = \frac{1}{2} p^\top M^{-1} p + \mathcal{V}_d$  denotes the desired Hamiltonian of the closed loop system that satisfies  $\operatorname{argmin}_{g_L} \mathcal{V}_d = g_d$  with  $g_L = g(L, \cdot)$ . Note that we omitted any damping injection since the material's intrinsic viscoelastic damping is deemed sufficiently large to guarantee stability. Following the concept of a kinematic feedback controller that artificially mimics an elastic element between the end-effector and the desired configuration in  $SE(3)$ , we choose the variation of the desired potential energy as follows

$$\frac{d\mathcal{V}_d}{dq} = \lambda_1 J^\top (J J^\top + \lambda_2 I)^{-1} \mathcal{F}_1, \quad (35)$$

where  $\lambda_1 > 0$  is a proportional gain,  $\lambda_2 > 0$  a controller gain related to the damping of the pseudo-inverse,  $\mathcal{F}_1 = k_p \log_{SE(3)}([g_L]_k^{-1} g_d)$  an artificial control wrench with positive definite matrix  $k_p$ , and  $\log_{SE(3)} : SE(3) \mapsto se(3)$  the logarithmic map. The controller gains  $\lambda_1$  and  $\lambda_2$  can be tuned accordingly to tweak the desired transient behavior of the closed-loop system, similar to a classical PD controller.

### 4 NUMERICAL STUDY CASE

In this section, we detail some numerical simulations using the proposed dynamic model in (33) together with the energy-shaping controller in (34). The truncation degree of the finite-dimensional model is  $k = 8$ . To simulate the under-actuation, we assume an input matrix  $G = \operatorname{blkdiag}\{I_3, O_5\}$  such that only the first three modes are actively controllable.

Table 1: Parameters setting for the numerical solver, the soft manipulator, and the energy-based controller.

Parameter description	Value
Undeformed length	$L = 120$ (mm)
Density	$\rho = 1250$ ( $\text{kgm}^{-3}$ )
Gravitational acceleration	$\gamma_g = 9.8$ ( $\text{ms}^{-2}$ )
Young's modulus	$E = 25$ (MPa)
Shear modulus	$\mu_1 = 10$ (MPa)
Constraint modulus	$\mu_2 = 15$ (GPa)
Rayleigh coefficient	$\zeta = 0.4$ (-)

Due to the partial differential nature, we have to employ a nested ODE routine to recover the trajectories for  $q$  and  $p$ . First, we employ an implicit trapezoidal solver with a fixed timestep of  $dt = 1$  ms to solve (33). At each time increment, we have to evaluate the dynamic matrices (17)-(22). To efficiently compute these dynamic entities, we solve the spatial integration problem over the material domain  $\mathbb{X}$  by using a second-order Runge-Kutta solver. The step-size for the spatial solver is  $d\sigma = 1$  mm. The open-source code is written in C++ and MATLAB, which is made publicly available at (Caasenbrood, 2020)

For soft material parameters, we choose an isotropic Hookean material with shear constraints. All the material properties related to the soft material are provided in Table 1. Given these material properties, the inertia tensor and the stiffness tensor become diagonal matrices:

$$\begin{aligned} \mathcal{M} &= \operatorname{blkdiag}\{\rho \mathcal{A}, \rho A, \rho A, \rho A\}, \\ \mathcal{K} &= \operatorname{blkdiag}\{\mu_1 \mathcal{A}, EA, \mu_2 A, \mu_2 A\}, \end{aligned}$$

where  $A > 0$  is the (average) cross-sectional area, and  $\mathcal{A}$  the second moment of area for a circular disc with radius  $R = 8$  mm. The damping tensor is chosen as  $\mathcal{D} = \zeta \mathcal{K}$  with damping coefficient  $\zeta$ . The generalized stiffness and damping matrix can then be pre-computed using (23) and (24).

As for control settings, the control gains are tuned to produce a smooth transient:  $\lambda_1 = 0.1$  and  $\lambda_2 = 0.01$ . The artificial spring stiffness is chosen as  $k_p = \operatorname{blkdiag}\{0.01 \cdot I_3, I_3\}$ . Lastly, the desired configuration of the end-effector is chosen as follows:

$$g_d = \begin{pmatrix} I_3 & r_d \\ 0_3^\top & 1 \end{pmatrix} \quad \text{with} \quad r_d = \begin{pmatrix} 0.05 \\ 0.00 \\ -0.01 \end{pmatrix}.$$

The simulation results for the closed-loop soft robotic system are shown in Figure 2 and Figure 3. Figure 2 shows the trajectories of the modal coefficients  $q(t)$  and the spatial trajectory of the end-effector of the soft robot, whereas Figure 3 has been provided to show the evolution of the continuous deformation of the soft robot. As can be seen, the

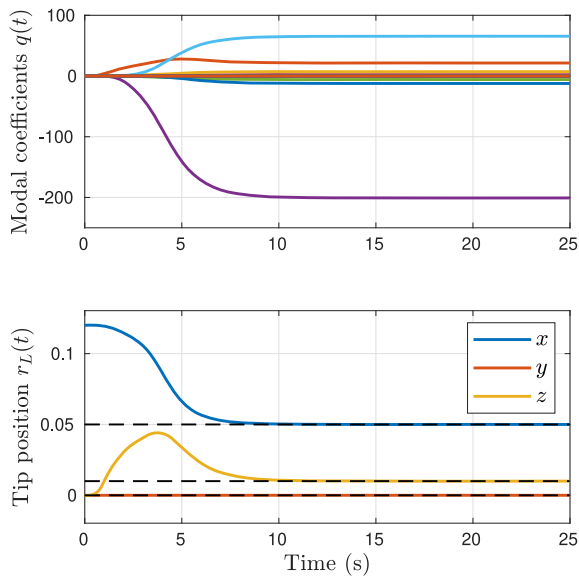


Figure 2: The evolution of the modal coefficients and the position of the end-effector of the soft robot manipulator.

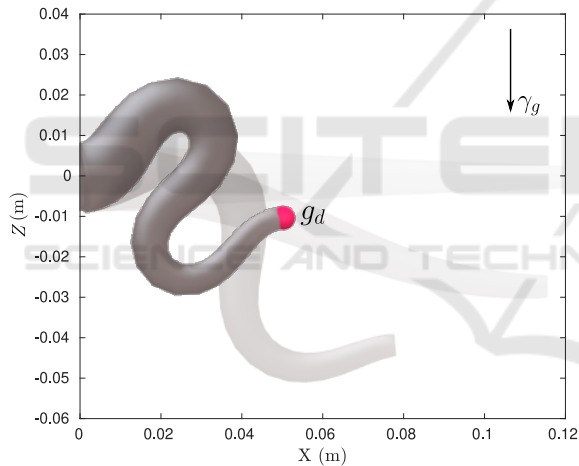


Figure 3: Three-dimensional evolution of the soft robot manipulators, slowly converging to the desired set-point  $g_d \in SE(3)$ .

end-effector of the soft robot manipulator slowly converges to the desired set-point  $g_d \in SE(3)$ . Although the control gains could be increased to promote a faster transient, it was observed that high gains lead to significant oscillations of the flexible structure. A possible solution might be to introduce negative damping to the controller Hamiltonian  $\mathcal{H}_d$ , to overcome the soft robot's structural damping.

## 5 CONCLUSION

The field of soft robotics is slowly maturing into a recognized subfield of robotics. Due to their intrinsic compliance, they allow for complex morphological motions that mimic animals in nature. Achieving similar performance to biology highlights the need for more accurate dynamic models and control strategies that fully exploit the hyper-redundant nature of soft robots. In this work, we provided a modeling framework for Cosserat beams that leads to a finite-dimensional system in a port-Hamiltonian structure. By exploiting the passivity, an energy-shaping controller was proposed that ensures the closed-loop Hamiltonian is minimal at the desired set-point. Inspired by an octopus, a numerical model was developed for a tentacle-like soft robot with distributed control inputs. The key challenges here regarding both the model as the controller are their ability to capture the hyper-flexibility, deal with intrinsic under-actuation, and exploit its hyper-redundancy to achieve its control task. Given appropriate controller gains, the model-based controller yields smooth convergence of the soft robot's end-effector while accounting for the intrinsic underactuated nature. Moreover, the mobility of the Cosserat model paired with the energy-based control has, to some extent, a resemblance to the biological motions seen in octopuses. Future work will focus on the following: *i*) validating the model and the controller experimentally, *ii*) adding hyper-elasticity, *iii*) constructing a set of basis functions through the so-called 'snapshot' decomposition method using FEM-driven data. In particular, the latter goal could be interesting to explore both advantages in FEM and Cosserat models, being accurate continuum deformations and computational efficiency, respectively.

## ACKNOWLEDGEMENTS

This work is partly supported by NWO, Netherlands Organization for Scientific Research; and is part of the Wearable Robotics perspective program. Website: [www.wearablerobotics.nl](http://www.wearablerobotics.nl).

## REFERENCES

- Astrid, P., Weiland, S., Willcox, K., and Backx, T. (2008). Missing point estimation in models described by proper orthogonal decomposition. *IEEE Transactions on Automatic Control*, 53(10):2237–2251.

- Boyer, F., Lebastard, V., Candelier, F., and Renda, F. (2020). Dynamics of continuum and soft robots: a strain parametrization based approach. *IEEE Transactions on Robotics*.
- Boyer, F., Porez, M., and Leroyer, A. (2010). Poincaré- Cosserat equations for the lighthill three-dimensional large amplitude elongated body theory: Application to robotics. 20(1):47–79.
- Caasenbrood, B. (2020). Sorotoki - an open-source soft robotics toolkit for matlab. <https://github.com/BJCaasenbrood/SorotokiCode>.
- Chirikjian, G. and Burdick, J. (1992). Kinematically optimal hyper-redundant manipulator configurations. *Proceedings 1992 IEEE International Conference on Robotics and Automation*.
- Choi, W., Whitesides, G. M., Wang, M., Chen, X., Shepherd, R. F., Mazzeo, A. D., Morin, S. A., Stokes, A. A., and Iliovski, F. (2011). Multigait soft robot. *Proceedings of the National Academy of Sciences*, 108(51):20400–20403.
- Della Santina, C. and Rus, D. (2020). Control oriented modeling of soft robots: The polynomial curvature case. *IEEE Robotics and Automation Letters*, 5(2):290–298.
- Duriez, C. (2013). Control of elastic soft robots based on real-time finite element method. *Proceedings - IEEE International Conference on Robotics and Automation*, pages 3982–3987.
- Falkenhahn, V., Mahl, T., Hildebrandt, A., Neumann, R., and Sawodny, O. (2015). Dynamic Modeling of Bellows-Actuated Continuum Robots Using the Euler-Lagrange Formalism. *IEEE Transactions on Robotics*, 31(6):1483–1496.
- Franco, E. and Garriga-Casanovas, A. (2020). Energy-shaping control of soft continuum manipulators with in-plane disturbances. *International Journal of Robotics Research*.
- Katzschmann, R. K., Della Santina, C. D., Toshimitsu, Y., Bicchi, A., and Rus, D. (2019). Dynamic motion control of multi-segment soft robots using piecewise constant curvature matched with an augmented rigid body model. *RoboSoft 2019 - 2019 IEEE International Conference on Soft Robotics*, (February):454–461.
- Kriegman, S., Blackiston, D., Levin, M., and Bongard, J. (2019). A scalable pipeline for designing reconfigurable organisms.
- Marchese, A. D., Onal, C. D., and Rus, D. (2014). Autonomous Soft Robotic Fish Capable of Escape Maneuvers Using Fluidic Elastomer Actuators. *Soft Robotics*, 1(1):75–87.
- Murray, R. M., Sastry, S. S., and Zexiang, L. (1994). *A Mathematical Introduction to Robotic Manipulation*. CRC Press, Inc., USA, 1st edition.
- Ortega, R., Spong, M. W., Gómez-Estern, F., and Blankenstein, G. (2002). Stabilization of a Class of Underactuated Mechanical Systems Via Interconnection and Damping Assignment. *IEEE Transactions on Automatic Control*, 47(8):1218–1233.
- Renda, F., Armanini, C., Lebastard, V., Candelier, F., and Boyer, F. (2020). A Geometric Variable-Strain Ap-

proach for Static Modeling of Soft Manipulators with Tendon and Fluidic Actuation. *IEEE Robotics and Automation Letters*, 5(3):4006–4013.

- Schaft, A. J. (2004). Port-Hamiltonian Systems: Network Modeling and Control of Nonlinear Physical Systems. *Advanced Dynamics and Control of Structures and Machines*, pages 127–167.
- Simo, J. C. and Vu-Quoc, L. (1986). A three-dimensional finite-strain rod model. part II: Computational aspects. *Computer Methods in Applied Mechanics and Engineering*, 58(1):79–116.
- Spong, M. W., Hutchinson, S., and Vidyasagar, M. (2006). *Robot modeling and control*. John Wiley & Sons, New York.
- Thuruthel, T., Falotico, E., Renda, F., and Laschi, C. (2018). Model-based reinforcement learning for closed-loop dynamic control of soft robotic manipulators. *IEEE Transactions on Robotics*, PP:1–11.
- Till, J., Aloï, V., and Rucker, C. (2019). Real-Time Dynamics of Soft and Continuum Robots based on Cosserat-Rod Real-Time Dynamics of Soft and Continuum Robots based on Cosserat-Rod Models. (May).
- Zhang, Z., Morales Bieze, T., Dequidt, J., Kruszewski, A., and Duriez, C. (2017). Visual Servoing Control of Soft Robots based on Finite Element Model. In *IROS 2017 - IEEE/RSJ International Conference on Intelligent Robots and Systems*, Vancouver, Canada.

## APPENDIX

### A. Deriving the Continuous Kinematics

Under Assumption 1, the configuration space of the soft robot  $g$  is everywhere differentiable. Then, using the equality of mixed partials, i.e.  $\frac{\partial}{\partial t}(\frac{\partial g}{\partial \sigma}) = \frac{\partial}{\partial \sigma}(\frac{\partial g}{\partial t})$ , we substitute  $\partial g / \partial t = g\hat{\eta}$  and  $\partial g / \partial \sigma = g\hat{\xi}$  to find

$$g\hat{\eta}\hat{\xi} + g\frac{\partial \hat{\xi}}{\partial t} = g\hat{\xi}\hat{\eta} + g\frac{\partial \hat{\eta}}{\partial \sigma}. \quad (36)$$

Pre-multiplying with  $g^{-1} \in SE(3)$  and rearranging the equality above, we obtain

$$\frac{\partial \hat{\eta}}{\partial \sigma} = -(\hat{\xi}\hat{\eta} - \hat{\eta}\hat{\xi}) + \dot{\hat{\xi}}, \quad (37)$$

where we can recognize the Lie bracket or the commutator between the vector fields  $\xi$  and  $\eta$  (Murray et al., 1994). Since the Lie bracket  $[\hat{\xi}, \hat{\eta}]$  itself also belongs to  $se(3)$ , which is isomorphic to  $\mathcal{R}^6$  via  $\hat{\eta} \mapsto \eta$ , we can rewrite the expressions as follows

$$\frac{\partial \eta}{\partial \sigma} = -\text{ad}_{\xi} \eta + \dot{\xi}, \quad (38)$$

where  $\text{ad}_{(\cdot)} : \mathcal{R}^6 \mapsto \mathcal{R}^{6 \times 6}$  defines the adjoint action map on the Lie algebra  $se(3)$ . This kinematic relation is analogous to (Boyer et al., 2020; Renda et al., 2020; Till et al., 2019)



## B. Partial Derivative of the Geometric Jacobian Matrix

The mapping from generalized coordinates  $\dot{q} \in \mathcal{R}^n$  to the velocity-twist vector  $\hat{\eta} = g^{-1}\dot{g} \in se(3) \cong \mathcal{R}^6$  for a point  $\sigma$  be given by  $\eta = J\dot{q}$  where  $J$  is the geometric Jacobian. The  $k$ -th order truncations of the exact geometric Jacobian is given by

$$[J]_k = \text{Ad}_{[g]_k}^{-1} \int_0^\sigma \text{Ad}_{[g]_k} \Theta d\sigma. \quad (39)$$

Again,  $\text{Ad}_{(\cdot)}$  above denotes the adjoint action on  $SE(3)$ . Unlike its notation in rigid robotics, note that the geometric Jacobian matrix here is time and space-variant. Following the chain rule of differentiation, the partial time-derivate of the geometric Jacobian matrix yields

$$[\dot{J}]_k = \left( \text{Ad}_{[g]_k}^{-1} \right) \int_0^\sigma \text{Ad}_{[g]_k} \Theta d\sigma + \text{Ad}_{[g]_k}^{-1} \int_0^\sigma (\dot{\text{Ad}}_{[g]_k}) \Theta d\sigma. \quad (40)$$

Given the differential relations of the adjoint action mapping on the Lie group, that is,  $d/ds(\text{Ad}_g) = \text{Ad}_g \text{ad}_\Upsilon$  given a twist  $\Upsilon = (g^{-1}dg/ds)^\vee$ , we can express the time-derivate of the adjoint action and its inverse as

$$\frac{\partial}{\partial t} (\text{Ad}_g) = \text{Ad}_g \text{ad}_\eta, \quad (41)$$

$$\frac{\partial}{\partial t} (\text{Ad}_{g^{-1}}) = -\text{ad}_\eta \text{Ad}_{g^{-1}}. \quad (42)$$

Substituting the truncated variations of (41) and (42) into (40), we find the complete expression of the time-derivate of the geometric Jacobian matrix

$$[\dot{J}]_k = -\text{ad}_\eta [J]_k + \text{Ad}_{[g]_k}^{-1} \int_0^\sigma \text{Ad}_{[g]_k} \text{ad}_{[\eta]_k} \Theta d\sigma. \quad (43)$$

Since  $\text{ad}_\eta(J\dot{q}) = \text{ad}_\eta \eta = 0_6$  by definition, the first right-hand term vanishes if (43) is post-multiplied with the generalized velocities  $\dot{q}$ , thus leading to the expression for the acceleration twist  $[\ddot{\eta}]_k$  in (13).